Journal of Photochemistry & Photobiology, B: Biology 283 (2026) 113551

Contents lists available at ScienceDirect

Journal of Photochemistry & Photobiology, B: Biology

journal homepage: www.elsevier.com/locate/jphotobiol

Targeting planktonic uropathogens and *Escherichia coli* biofilm with photodynamic therapy mediated by methylene blue and potassium iodide

Daniela Silva [a], Inês Mendonça [a], Cátia Vieira [a], M. Graça P.M.S. Neves [b], M. Amparo Faustino [b,*], Maria Bartolomeu [a,c], Adelaide Almeida [a,*]

[a] Department of Biology & CESAM, University of Aveiro, 3810-193 Aveiro, Portugal
[b] Department of Chemistry & LAQV-REQUIMTE, University of Aveiro, 3810-193 Aveiro, Portugal
[c] Centre for Interdisciplinary Research in Health (CIIS), Universidade Católica Portuguesa, Faculty of Dental Medicine, 3504-505 Viseu, Portugal

ARTICLE INFO

Keywords:
Urinary tract infections
Antimicrobial photodynamic therapy
Methylene blue, polymicrobial
Escherichia coli
Enterococcus faecalis
Klebsiella pneumoniae
Proteus mirabilis
Pseudomonas aeruginosa
Planktonic bacteria
Biofilms
Catheters

ABSTRACT

Urinary tract infections (UTIs) are among the most common infections worldwide, with many hospital-acquired cases linked to biofilm formation on urinary catheter surfaces. The growing problem of antimicrobial resistance limits the effectiveness of conventional antibiotics, and antimicrobial photodynamic therapy (aPDT) has emerged as a promising alternative. This approach is based on the combination of a photosensitizer (PS), dioxygen, and visible light to reduce bacterial concentration without promoting resistance. In this study, the potential of aPDT in controlling UTIs was evaluated using a well-studied PS, methylene blue (**MB**), alone or in the presence of potassium iodide (KI). *Ex vivo* assays in urine were conducted using the five most common UTI-causing bacteria: *Klebsiella pneumoniae*, *Escherichia coli*, *Enterococcus faecalis*, *Proteus mirabilis*, and *Pseudomonas aeruginosa*. **MB** alone effectively photoinactivated *E. coli, P. mirabilis,* and *E. faecalis* in planktonic form, with limited activity against *K. pneumoniae* and *P. aeruginosa*. The addition of KI significantly enhanced the photodynamic effect against all tested strains, resulting in a reduced treatment time, and was also effective against mixed bacterial populations in the planktonic state. The efficacy of the treatments was further evaluated against *E. coli* cells within biofilms formed on urinary catheter surfaces. The combined action of **MB** and KI successfully controlled *E. coli* biofilms, achieving reductions of 3.9 (> 99.987%) and 6.0 $\log_{10}$ CFU mL^{-1} after one and two aPDT treatment cycles, respectively. Overall, these findings highlight **MB** + KI-mediated aPDT as a promising strategy for the photoinactivation of planktonic uropathogens and *E. coli* biofilms formed on urinary catheter surfaces.

1. Introduction

Currently, urinary tract infections (UTIs) are one of the most common bacterial infections in humans [1], affecting around 150 million people worldwide each year [2,3]. These infections can be acquired both in the community [2] and at hospital levels [4]. *Escherichia coli* is the microorganism most associated with urinary tract infections, being responsible for approximately 70–80% of community-acquired infections [5,6]. In addition to *E. coli*, there are other bacteria frequently associated with UTIs, such as *Klebsiella pneumoniae*, *Proteus mirabilis*, *Enterococcus faecalis*, and *Pseudomonas aeruginosa* [1,3,7].

The use of medical devices, such as urinary catheters, constitutes a risk factor for the occurrence of UTIs, being responsible for 75% of the UTIs in hospitals [8]. Biofilm formation on the surface of urinary catheters plays a key role in the pathogenesis of catheter-associated UTIs (CAUTIs) [9,10]. Biofilms are well-organized and structured communities of microorganisms encapsulated in a self-generated extracellular polymeric matrix, which easily adheres to surfaces. This extracellular polymeric matrix acts as a physical barrier to antimicrobial agents, protecting microorganisms and making them more resistant to elimination. Thus, biofilms are less susceptible to antimicrobial treatments than the corresponding planktonic bacteria [9,10], with uropathogenic *E. coli* (UPEC) being one of the main causative agents of CAUTIs [9].

Although UTIs are commonly treated with conventional antibiotics, their frequent and inappropriate use has contributed to an increased incidence of multidrug-resistant bacteria, thus limiting treatment options [11–14]. Therefore, there is a growing need to develop new antimicrobial approaches for these infections.

In recent years, antimicrobial photodynamic therapy (aPDT) has proven to be an effective approach in inactivating microorganisms,

* Corresponding authors.
E-mail addresses: faustino@ua.pt (M.A. Faustino), aalmeida@ua.pt (A. Almeida).

https://doi.org/10.1016/j.jphotobiol.2026.113551
Received 18 March 2026; Received in revised form 10 August 2026; Accepted 26 August 2026
Available online 27 August 2026

representing a promising alternative to conventional treatments [14]. This approach requires activation of the photosensitizer (PS) by visible light in the presence of dioxygen ($^3O_2$) to generate reactive oxygen species (ROS), such as singlet oxygen ($^1O_2$). These cytotoxic species oxidize biomolecules in bacterial cells (*e.g.,* proteins, nucleic acids, lipids), leading to microbial lysis and cell death [15–17]. This approach offers several advantages when compared to conventional antibiotics: i) it is efficient regardless of the microorganism's antibiotic resistance profile [18]; ii) it does not induce resistance, even after several cycles of aPDT treatment [16,19]; and iii) it is effective against Gram-negative and Gram-positive bacteria [16,20,21]. It is generally accepted that this approach is more effective against Gram-positive bacteria due to their highly permeable cell walls. In contrast, the outer membrane of Gram-negative bacteria limits PS interaction and reduces photodynamic efficacy [22–24]. Nevertheless, rational PS design, such as introducing positive charges on its core or combining it with adjuvants, can enhance uptake and overcome these limitations. Previous studies have shown that combining certain PS with inorganic salts, such as potassium iodide (KI), can enhance the efficiency of aPDT [25–28], resulting in higher inactivation rates than with the PS alone [26,29–31]. This synergistic effect is caused by the initial production of peroxyiodide ($HOOI_2^-$) as a result of the interaction of KI with $^1O_2$ produced by PS. Then, $HOOI_2^-$ may undergo further degradation into cytotoxic species such as free iodine/tri-iodine ion (I_2/I_3^-) and hydrogen peroxide (H_2O_2) or iodine radicals ($I_2^{\bullet-}$) [27,29,32–34].

Evidence from several studies suggests that aPDT may be an effective strategy for treating UTIs, including infections caused by Gram-negative bacteria [15,27]. In 2015, Liu et al. demonstrated that polymeric nanoparticles encapsulated with chlorin e_6 (**Ce$_6$**; 200 μM) are effective in treating bladder infections in mice caused by *E. coli*, upon irradiation of the bladder with red light (664 nm; 50 mW cm^{-2}; 90 J cm^{-2}) [35]. Similarly, another study reported high success in treating rats infected with *E. coli* using **MB** in combination with KI under intravesical red-light illumination (660 nm; 50 mW cm^{-2}; 100 J cm^{-2}) [32]. In addition to its therapeutic potential in urinary infections, aPDT has also been shown to be effective in disinfecting urinary catheters [8]. For instance, Santos and co-workers demonstrated that the external application of a tetracationic porphyrin–cisplatin complex (**3-*cis*-PtTPyP**) effectively inhibited *Proteus mirabilis* biofilms on urinary catheters [36]. Furthermore, other studies have reported that incorporating PS into catheter materials, such as toluidine blue (**TBO**), hypericin-containing liposomes, **MB**@Au nanoparticles, and sodium copper chlorophyllin, can effectively destroy biofilms [37–40]. Taken together, these findings suggest that aPDT may be a promising approach not only for the treatment but also for the prevention of UTIs. While several studies have already demonstrated the efficacy of aPDT in UTI, important gaps remain regarding its performance in clinically relevant conditions and against polymicrobial infections.

Although **MB** combined with KI was effective in a rat UTI model of *E. coli*-induced UTI [32], its activity against a broader clinically relevant uropathogens, under polymicrobial conditions, and in the context of catheter disinfection, remains unexplored. UTIs are frequently polymicrobial [41,42], and catheter-associated infections represent a particularly challenging clinical scenario due to both the structural complexity of mature biofilms and the interference of the organic matrix inherent to human urine [27,32,43].

We hypothesized that combining **MB** with KI would generate long-lived reactive iodine species (RIS) capable of overcoming these bottlenecks and achieving effective bacterial photoinactivation in a clinically relevant medium. The objective of this *ex vivo* proof-of-concept study was to evaluate **MB**-mediated aPDT, with and without KI, against the five uropathogens most frequently associated with UTIs (*K. pneumoniae, E. coli, E. faecalis, P. mirabilis, and P. aeruginosa*) [1,3,7]. Considering that UTIs can be polymicrobial [40,41], assays were carried out using both mono-species cultures and a mixed bacterial consortium in the planktonic state. Furthermore, the potential of aPDT to inactivate *E. coli* cells within biofilms formed on urinary catheters was also investigated, as *E. coli* remains the most prevalent uropathogen associated with UTIs. Overall, this study aims to assess whether **MB**/KI-based aPDT holds promise as an alternative to antibiotics for UTI management.

2. Materials and methods

The experimental design adopted in this study is summarized in Fig. 1.

2.1. Photosensitizer and KI solutions

MB was purchased from Acros Organics (Geel, Antwerpen, Belgium), and a stock solution of **MB** was prepared in phosphate-buffered saline (PBS) at a concentration of 500 μM. Before each assay, the **MB** stock solution was sonicated in the dark for 30 min to homogenize. Potassium iodide was purchased from Sigma-Aldrich (St. Louis, MO), and KI working solutions were prepared at 5.0 M in sterile PBS immediately before each experiment.

2.2. Light source

The effect of aPDT with **MB**, alone and in combination with KI, was evaluated by exposing the samples to white light irradiation (400–700 nm) from an LED system (LUMECO, 30 W, 2000 lm) at an irradiance of 50 mW cm^{-2}. A broad-spectrum white LED was selected because its emission spectrum contains a substantial red component that overlaps with the absorption band of **MB**, allowing effective photoactivation while providing a simple, inexpensive, and widely available light source. The total light irradiance (400 to 700 nm) was measured using a Coherent FieldMax II-Top Power Meter combined with a Coherent PowerSens PS19Q. Based on the spectral overlap between the emission spectrum of the LED system used and the absorption spectrum of **MB**, calculated according to the Light Dose Correction (LDC) method [44], the effective light irradiance absorbed by the **MB** was estimated at 15.5 mW cm^{-2} [29] to achive the expected light irradiation. The distance between the LED source and the samples was 6.8 cm, and all samples were positioned centrally beneath the light source to ensure uniform illumination across the irradiated area.

2.3. Bacterial strains and growth conditions

The five bacteria used in this study were *Escherichia coli* ATCC 25922, *Enterococcus faecalis* ATCC 29212, *Proteus mirabilis* DSM 102258, *Klebsiella pneumoniae* SCC1 (from wastewater [45]), and *Pseudomonas aeruginosa* (from a patient's exudates at Pedro Hispano Hospital [46]). The bacterial streaks were made on Tryptic Soy Agar (TSA; Liofilchem, Italy) and kept at 4 °C. Before each assay, three isolated colonies were inoculated into 30 mL of Tryptic Soy Broth (TSB; Liofilchem, Italy) and incubated at 37 °C for 18 to 24 h, under stirring (120 rpm). After this period, an aliquot of the culture (300 μL) was transferred to fresh TSB (30 mL) and incubated under the previously described growth conditions until the stationary growth phase was reached, corresponding to a concentration of approximately 10^9 colony-forming units per mL (9 $\log_{10}$ CFU mL^{-1}) [27,46]. This culture corresponds to the bacterial suspension used in bacterial inactivation assays.

2.4. Photodynamic inactivation assays of planktonic cells

2.4.1. Photoinactivation assays in PBS (in vitro studies)

To select the best conditions to use posteriorly in the human urine *ex vivo* assays, preliminary *in vitro* assays were performed in PBS using *P. aeruginosa*. This strain was specifically selected for the initial *in vitro* screening in PBS because it is widely described in the literature as one of the uropathogens with the lowest inherent susceptibility to aPDT. Ensuring optimization parameters (PS concentration and KI adjuvant

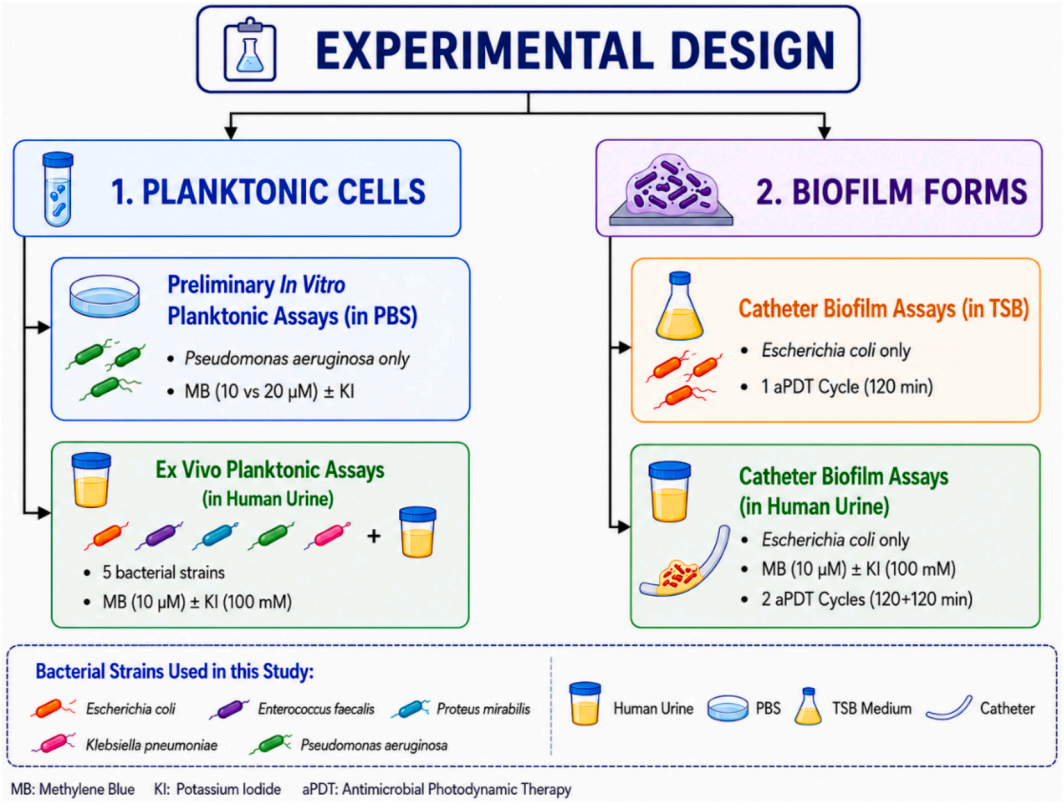

Fig. 1. Schematic illustration of the experimental design used to evaluate mediated **MB**-aPDT with and without KI against uropathogens in planktonic forms (preliminary *in vitro* PBS assays and *ex vivo* studies in human urine) and mature biofilms formed on urinary catheters in both TSB medium and human urine.

matching) on this highly resilient strain allowed us to establish a conservative and robust foundation for all subsequent assays [47–50]. These assays were performed with two concentrations of **MB**, 10 and 20 µM, and in both cases, the photodynamic action under white light irradiation at an effective irradiance of 15.5 mW cm^{-2} was tested with and without the addition of KI at 100 mM. This concentration of KI was selected based on previous studies demonstrating its effectiveness in enhancing the aPDT effect without affecting bacterial viability [27,32,43,47,51].

Based on these conditions, a bacterial culture in the stationary phase was diluted in PBS (1:10) and transferred to 12-well plates. Then, appropriate volumes of **MB** or **MB** with KI were added to achieve the desired final concentrations. All experiments also included light and dark controls to ensure the reliability of the results. Two light controls, containing the bacterial suspension alone (LC) or with KI (LC + KI), were exposed to the same light conditions to evaluate the effect of light on bacterial viability. A dark control (DC), containing the bacterial suspension with **MB** at the highest tested concentration (20 µM) and KI (100 mM), was protected from light to assess the cytotoxicity of **MB** and KI in the dark.

After preparing the samples and controls, the plates were incubated in the dark for 15 min at 25 °C under agitation (120 rpm) to promote the binding of **MB** to bacterial cells. After this period, the plates containing the samples and light controls were irradiated, under agitation, for 120 min. In turn, dark controls were protected from light during the irradiation period. Aliquots (100 µL) of samples and controls were collected after the incubation period in the dark (time 0) and during irradiation. Then, aliquots were serially diluted tenfold in PBS from 10^{-1} down to 10^{-6} to ensure accurate colony counting within the reliable dynamic range of the drop-plate method. For each dilution, two drops (10 µL each) were plated in TSA. After the drops dried, the Petri dishes were inverted and incubated at 37 °C for 18 to 24 h. Colonies were counted at the most appropriate dilution, and the concentration of viable cells was expressed as $\log_{10}$ CFU mL^{-1}. Three independent biological assays were performed, each with two replicates. Averages were calculated from the three assays.

2.4.2. *Urine photoinactivation assays (ex vivo studies)*

The optimal inactivation conditions identified in preliminary assays (**MB** at 10 µM, with and without KI at 100 mM) were selected for urine assays. Under these conditions, the effectiveness of aPDT treatments was evaluated against each of the five bacteria individually (*E. coli*, *K. pneumoniae*, *P. mirabilis*, *E. faecalis,* and *P. aeruginosa*), as well as against a mixed culture containing all strains. For the mixed-bacteria assays, equal volumes (40 µL) of each bacterial suspension in the stationary growth phase were combined and diluted at a 1:10 ratio in urine before being transferred to 12-well plates.

The assays followed the same protocol for the *in vitro* assays (Section 2.4.1) but used fresh urine as the experimental medium in place of PBS. Human urine samples were collected in the morning on the day of each experiment *via* midstream clean-catch technique from a single healthy human volunteer donor with no history of active urinary pathology or recent consumption of antimicrobial agents. The urine samples were not subjected to any sterilization procedures prior to the experiments. To monitor potential endogenous microbial contamination, a urine-only negative control (urine without bacterial inoculation) was included in each assay and processed under the same experimental conditions. The samples were fully anonymized, non-traceable, and processed immediately on-site, in accordance with the institutional ethical compliance guidelines of the University of Aveiro. The pH of each urine sample was recorded. Alongside the samples, light and dark controls were carried out as previously described (Section 2.4.1).

2.5. Photodynamic inactivation assays of E. coli biofilms formed in urinary catheters

The effect of aPDT on the photoinactivation of *E. coli* biofilms was evaluated on urinary catheters. This Gram-negative bacterium was selected as the sole target for catheter assays due to its overwhelming clinical and epidemiological dominance, being responsible for up to 80% of UTIs and acting as the primary agent in catheter-associated urinary tract infections (CAUTIs) [5,6,9]. The initial tests were carried out on *E. coli* biofilms formed under ideal conditions (in TSB culture medium), using **MB** (10 μM) alone and in combination with KI (100 mM). Posteriorly, the effectiveness of these aPDT treatments was assessed on biofilms formed in urine on urinary catheters, providing a more physiologically relevant *ex vivo* model than standard *in vitro* assays.

2.5.1. Preparation of urinary catheters

Sterile urinary catheters were purchased from Aveimédica (Aveiro, Portugal) and, under aseptic conditions, cut transversely into 3 cm sections that were subsequently transferred to 6-well plates. For each collection time, two plates with urinary catheters were prepared, one containing the irradiated samples and light controls (LC and LC + KI) and the other containing the dark control (DC + KI).

2.5.2. Formation of biofilms in urinary catheters

A bacterial suspension (300 μL) in the stationary growth phase was centrifuged at 10,000 rpm for 5 min (Megafuge 16R, Thermo Scientific). Subsequently, the supernatant was removed, and the pellet was resuspended in TSB or fresh urine (30 mL). Then, 200 μL of the previous suspension was transferred to the central part of the interior of each previously prepared catheter section and placed in 6-well plates. The plates were wrapped in sterile cling film to prevent evaporation of the culture medium and incubated at 37 °C for 24 h. The following day, the culture medium was carefully replaced without disrupting the preformed biofilm, and the samples were incubated again under the previously described conditions. After a total of 48 h of biofilm growth, the mature biofilm formed in TSB or urine was used in the following assays.

2.5.3. Photodynamic inactivation of E. coli in biofilms formed in TSB

After biofilm growth on the urinary catheter, each section was washed three times with 1 mL of PBS to remove planktonic cells. Separately, solutions of **MB** and/or **MB** + KI were prepared in PBS at the desired concentrations (**MB** at 10 μM, KI at 100 mM) and transferred (200 μL) to the central part of the interior of each catheter section containing the biofilm. Simultaneously, the same controls previously described for suspension assays were also performed (LC, LC + KI, DC + KI). In light controls, 200 μL of PBS alone (LC) or PBS with KI (LC + KI) were added; for dark controls, 200 μL of the previously prepared **MB** or **MB** + KI solutions were added. For each independent assay, 2 catheter sections were used for each sample and control. After preparing the samples and controls, the plates containing the catheters were subsequently incubated in the dark for 30 min at 25 °C to promote the binding of **MB** to the bacterial cells. After this period, biofilms present in the urinary catheter corresponding to the initial time (time 0) were quantified. Simultaneously, the plate containing the urinary catheter corresponding to the samples and light controls was irradiated for 120 min with an effective light irradiance of 15.5 mW cm^{-2}. In parallel, the plates containing the dark controls (DC) were protected from the light for the same period.

2.5.4. Photodynamic inactivation of E. coli in biofilms formed in urine

For aPDT treatment in the E. coli biofilm assays in urine, two aPDT treatment cycles were performed. The first aPDT cycle followed the procedure previously described for biofilms formed in TSB. In the second aPDT cycle, an additional 200 μL of **MB** or **MB** + KI previously prepared solution was added to previously treated catheter sections, followed by irradiation. For light controls, second doses of 200 μL PBS or PBS + KI were also added to LC and LC + KI, respectively, while no addition was performed for dark controls (DC), which were kept in the absence of light, and no photobleaching was observed.

2.5.5. Quantification of biofilms

To quantify the biofilm, bacterial cells from the catheters were collected using a swab-based method adapted from previously reported protocols for catheter-associated biofilms [52,53]. Before establishing this protocol, three biofilm recovery methods were compared using catheter segments: (i) swabbing the catheter surface using a standardized procedure, (ii) detaching the biofilm by vortexing, and (iii) detaching the biofilm by ultrasonic bath treatment. Under our experimental conditions, the swabbing method consistently recovered a higher quantity of biofilm-associated cells than the vortexing and ultrasonic bath procedures and was therefore selected for all subsequent assays. All swabbing procedures were performed by the same operator following the same standardized protocol to minimize variability. To do this, the swab was dipped in PBS (1.0 mL), contained in a microtube (one for each section), and rubbed against the catheter 3 times. Then, the swab was washed in the corresponding microtube and squeezed against the inner walls of the microtube at the end, so that the liquid containing the cells remained in the tube. This process was repeated 10 times in total for each section to ensure the maximum number of bacterial cells were collected. The samples collected in microtubes were homogenized by vortexing, serially diluted in PBS, plated, and incubated as described above. Three independent assays were carried out, with four replicates per assay. The average of the results obtained in the different tests was calculated. The results were expressed as $\log_{10}$ CFU mL^{-1}.

2.6. Statistical analysis

Statistical analysis was performed using data obtained from three independent biological assays (conducted on different days), with each sample analyzed in technical duplicates (for planktonic cells) and quadruplets (for biofilms). Data processing and statistical evaluations were conducted using the GraphPad Prism 7.04 software. Normal distributions were verified with the Kolmogorov-Smirnov test, and homogeneity of variance was assessed with the Brown-Forsythe test. Two-way ANOVA analysis of variance and Tukey's multiple comparison test were applied to evaluate the significance of differences between the tested conditions. Differences corresponding to $p < 0.05$ were considered significant.

3. Results

3.1. In vitro photoinactivation assays

A preliminary evaluation of the most effective aPDT conditions for subsequent *ex-vivo* experiments was carried out with *P. aeruginosa* in PBS. These *in vitro* assays were performed with **MB** at two concentrations (10 and 20 μM) under white light irradiation at an effective irradiance of 15.5 mW cm^{-2}, both in the absence of KI (Fig. 2a) and in its presence (100 mM of KI) (Fig. 2b).

In all assays, the bacterial concentration in the controls (LC and DC) did not show significant variation (ANOVA, $p > 0.05$), indicating that *P. aeruginosa* cell viability was not significantly affected by irradiation (LC), the presence of KI under irradiation (LC + KI), PS alone in the absence of light (DC), or with KI (DC + KI), even at the highest tested concentration (20 μM **MB** and 20 μM **MB** + 100 mM KI).

The *P. aeruginosa* inactivation obtained after aPDT with **MB** alone (Fig. 2a) indicated that its photodynamic effect was not significantly dependent on the tested concentrations (ANOVA, $p > 0.05$). After 45 min of aPDT treatment, bacterial concentrations were reduced by 3.9 $\log_{10}$ CFU mL^{-1} (ANOVA, $p < 0.0001$) with **MB** at a concentration of 10 μM and by 4.3 $\log_{10}$ CFU mL^{-1} (ANOVA, $p < 0.0001$) with **MB** at 20 μM.

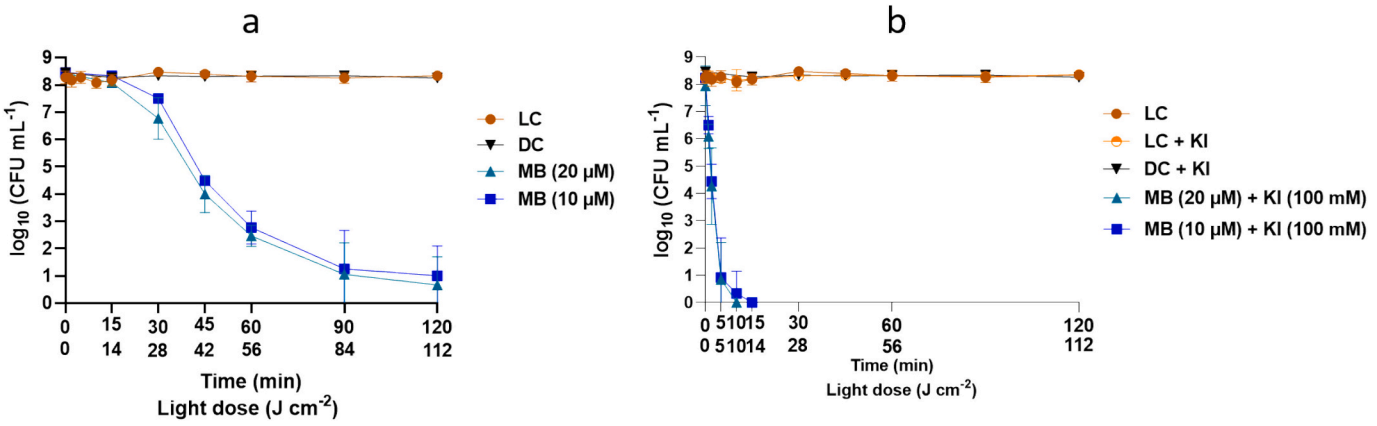

Fig. 2. Photodynamic inactivation of *P. aeruginosa* using **MB** at 10 and 20 μM, in the absence (a) and in the presence of KI at 100 mM (b), under white light irradiation at an effective irradiance of 15.5 mW cm^{-2} for 120 min (total light dose of 112 J cm^{-2}). Values are presented as the means of three independent assays in duplicate; standard deviation is represented by error bars. LC: light control; DC: dark control.

After 120 min of irradiation, the bacterial photoinactivation reached 7.3 Log_{10} CFU mL^{-1} (ANOVA, $p < 0.0001$) and 7.6 log_{10} CFU mL^{-1} (ANOVA, $p < 0.0001$) in the assays with **MB** at 10 and 20 μM, respectively.

The combined use of **MB** with KI significantly enhanced the PS's photodynamic effect (ANOVA, $p < 0.05$), resulting in an abrupt bacterial inactivation profile (Fig. 2b). With **MB** at 10 μM in the presence of KI, a bacterial reduction of 3.7 Log_{10} CFU mL^{-1} (ANOVA, $p < 0.0001$) was achieved after just 2 min of white light irradiation, reaching the detection limit of the method (*ca.* 8.0 Log_{10} CFU mL^{-1} reduction) after 15 min (ANOVA, $p < 0.0001$) (Fig. 2b). With **MB** at 20 μM, bacterial photoinactivation of 3.9 Log_{10} CFU mL^{-1} (ANOVA, $p < 0.05$) occurred after 2 min, and the detection limit of the method was reached after 10 min (ANOVA, $p < 0.0001$) (Fig. 2b).

Since the aPDT results obtained for the two tested concentrations were not significantly different, the conditions selected for the subsequent aPDT experiments were **MB** at a concentration of 10 μM without and with KI at 100 mM under white light irradiation at an effective light irradiance of 15.5 mW cm^{-2}.

3.2. *Ex vivo photoinactivation assays of individual bacterium in urine*

After the establishment of the most effective aPDT conditions, the photodynamic effect of **MB** (10 μM), alone and combined with KI, was investigated against the most prevalent uropathogenic bacterial strains (*E. coli*, *K. pneumoniae*, *P. mirabilis*, *E. faecalis,* and *P. aeruginosa*) in urine, both individually and in a bacterial mixture. Although the preliminary evaluation indicated that **MB** performed better in the presence of KI, these analyses were also carried out in its absence. This decision was based on the higher chemical complexity of urine compared with PBS, which may influence the aPDT outcomes.

The results summarized in Figs. 3 and 4 (*vide infra*) show no significant variations on the bacterial abundance in light (LC and LC + KI) and dark controls (DC) (ANOVA, $p > 0.05$), confirming the reliability of the photoinactivation assays and the absence of toxicity from KI under irradiation (LC + KI), and from the **MB** + KI combination in the dark (DC and DC + KI).

The results of the aPDT treatments (**MB** and **MB** + KI) toward each selected bacterium are represented in Fig. 3. Overall, *P. aeruginosa* was the least susceptible bacterial species to aPDT treatments, followed by *K. pneumoniae*, *E. coli*, and *P. mirabilis* (Gram-negative bacteria). The *E. faecalis* (a Gram-positive bacterium) exhibited the highest susceptibility to the aPDT treatment.

aPDT treatments in urine with **MB** alone had limited efficiency, particularly against *P. aeruginosa* (0.57 log_{10} CFU mL^{-1}, ANOVA, $p > 0.05$) and *K. pneumoniae* (0.73 log_{10} CFU mL^{-1}, ANOVA, $p < 0.05$) (Fig. 3a and b) after 120 min of light irradiation. On the other hand, a more efficient photoinactivation was observed for *E. coli*, *P. mirabilis,* and *E. faecalis*. For *E. coli*, **MB** promoted a significant reduction of 3.2 log_{10} CFU mL^{-1} (ANOVA, $p < 0.0001$) after 120 min of aPDT treatment (Fig. 3c). In the cases of *P. mirabilis* and *E. faecalis*, bacterial reductions of 5.0 log_{10} CFU mL^{-1} and 6.4 log_{10} CFU mL^{-1}, respectively, were achieved after 60 min of aPDT treatment, and photoinactivation to the detection limit of the method (*ca.* 8.0 log_{10} CFU mL^{-1} reduction) was observed after doubling the light exposure time to 120 min (Fig. 3d and e).

Compared to aPDT treatments with **MB** alone, the combination of **MB** + KI was more effective in inactivating all bacteria studied, resulting in faster and more substantial inactivation across all strains (ANOVA, $p < 0.05$). For *P. aeruginosa,* a significant reduction of 4.4 log_{10} CFU mL^{-1} (ANOVA, $p < 0.0001$) was observed after 120 min of combined aPDT-KI treatment (Fig. 3a). *K. pneumoniae* and *E. coli* reached the detection limit of the method (*ca.* 8.0 log_{10} CFU mL^{-1} reduction; ANOVA, $p < 0.0001$) within 90 and 60 min, respectively (Fig. 3b and c). The presence of KI also has a pronounced effect on light exposure time required to reach the detection limit of the method, reducing it by half for *P. mirabilis* (from 120 to 60 min) and by nearly eightfold for *E. faecalis* (from 120 to 15 min) (Fig. 3d and e).

Because fresh urine was used without prior sterilization, a urine-only negative control was included in each experiment to assess potential endogenous microbial contamination. No bacterial colonies were detected in these controls (data not shown), indicating that any endogenous microorganisms present in the urine samples were below the detection limit of the culture method used (2 log CFU mL^{-1}).

3.3. *Ex vivo photoinactivation of a mixture of the five bacteria in urine*

The effect of aPDT treatments on urine was also evaluated using a consortium of the five selected bacterial strains, given that urinary tract infections, although less frequently polymicrobial than other infection types, can involve multiple infectious agents simultaneously [41,42]. The results, shown in Fig. 4, indicate that the aPDT treatment mediated by **MB** alone promoted a significant reduction in the total number of viable cells, with a decrease of 3.1 log_{10} CFU mL^{-1} (>99.9% of bacterial reduction, ANOVA, $p < 0.0001$) after 120 min of treatment. On the other hand, the combined **MB** + KI aPDT treatment led to a more pronounced bacterial inactivation, reaching the detection limit of the method (reduction of 8.1 log_{10} CFU mL^{-1}) after 90 min of white light irradiation (ANOVA, $p < 0.0001$) (Fig. 4).

3.4. *Photoinactivation assays of E. coli biofilms in urinary catheters*

To further assess the potential of the aPDT treatments, the effects of

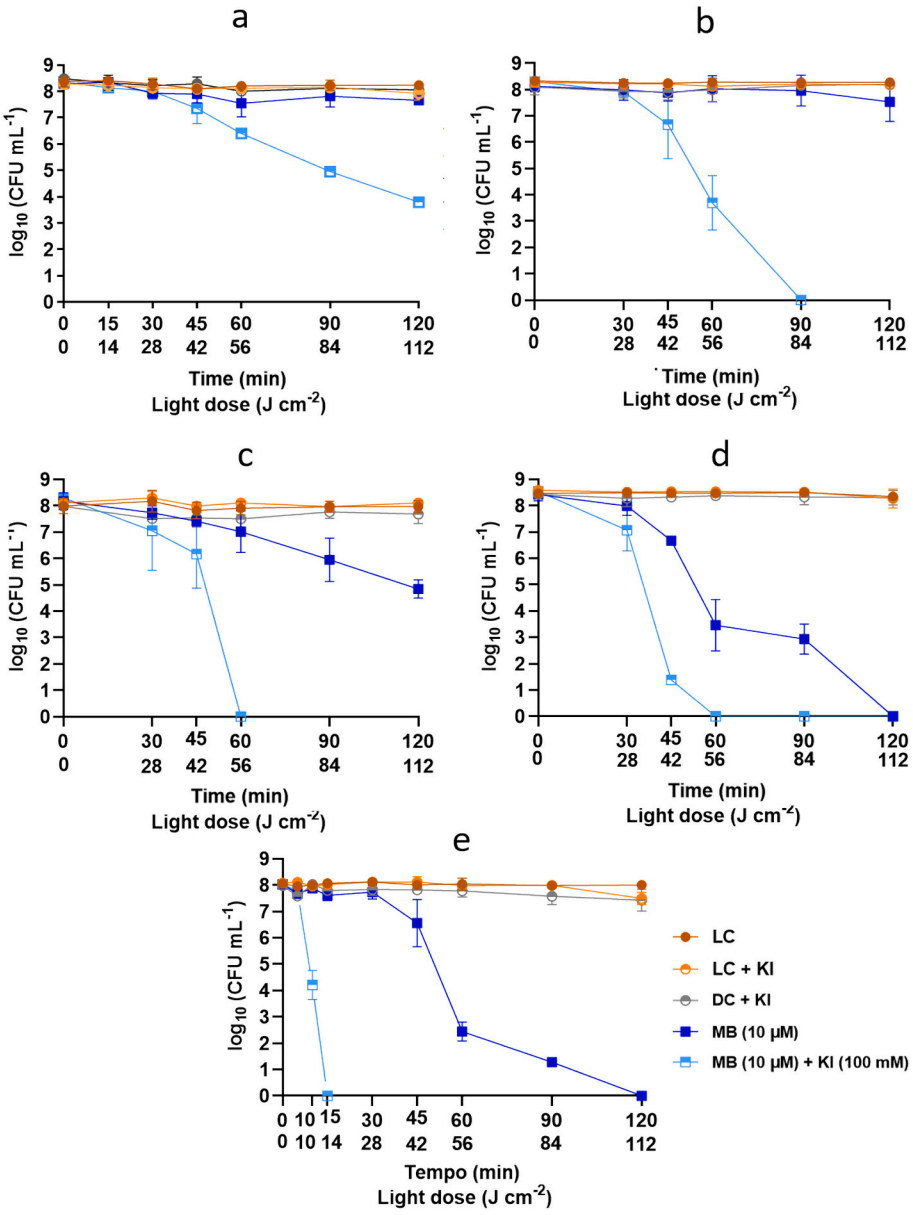

Fig. 3. Photodynamic inactivation of *P. aeruginosa* (a), *K. pneumoniae* (b), *E. coli* (c), *P. mirabilis* (d), *E. faecalis* (e) in urine, mediated by **MB** at 10 µM, in the presence and in the absence of KI at 100 mM, under white light irradiation at an effective light irradiance of 15.5 mW cm^{-2} for 120 min (total light dose of 112 J cm^{-2}) Values are presented as the means of three independent assays in duplicate; standard deviation is represented by error bars. LC: light control; DC: dark control.

photodynamic action on the photoinactivation of *E. coli* biofilms in urinary catheters were evaluated. This Gram-negative bacterium was selected as the most common strain associated with UTIs, particularly on urinary catheters. The initial experiments were carried out on *E. coli* biofilms formed under ideal growth conditions (in TSB), using **MB** alone or in combination with KI. Then, the efficacy of these aPDT treatments was evaluated on biofilms formed in urine on urinary catheters, providing a more physiologically relevant *ex vivo* model than standard *in vitro* assays. These aPDT assays were also performed with **MB** at 10 µM alone and in combination with KI, under irradiation with white light (effective light irradiance of 15.5 mW cm^{-2}).

In all assays, the bacterial concentration of all controls did not vary significantly ($p > 0.05$), indicating that the irradiation alone (LC), KI under white light irradiation (LC + KI) and **MB** + KI combination in the dark (DC + KI) did not affect the viability of *E. coli* biofilms, as shown in Figs. 5 and 6.

3.4.1. Photodynamic inactivation of E. coli biofilms grown in TSB

The results summarized in Fig. 5a show that aPDT treatments of *E. coli* biofilms grown in TSB with **MB** alone reduced the bacterial counts by 3.0 $\log_{10}$ CFU mL^{-1} (99.9% reduction ANOVA, $p < 0.0001$) after 120 min of light exposure. In assays mediated by **MB** + KI, this bacterial biofilm reduction doubled to 6.0 $\log_{10}$ CFU mL^{-1} (99.9999%, ANOVA, $p < 0.0001$) over the same irradiation period (120 min). Progressive photobleaching of **MB** was observed over the course of white-light irradiation (Fig. 5b).

3.4.2. Photodynamic inactivation of E. coli biofilms grown in urine

The results summarized in Fig. 6 show that the efficiency of the aPDT treatments on *E. coli* biofilms grown in urine is maximized after two consecutive aPDT treatment cycles. Two aPDT cycles (120 min each) were applied to overcome **MB** photobleaching observed in previous TSB medium assays. With **MB** alone, *E. coli* reductions of 2.1 and 3.4 $\log_{10}$ CFU mL^{-1} were achieved after the first and second aPDT cycles,

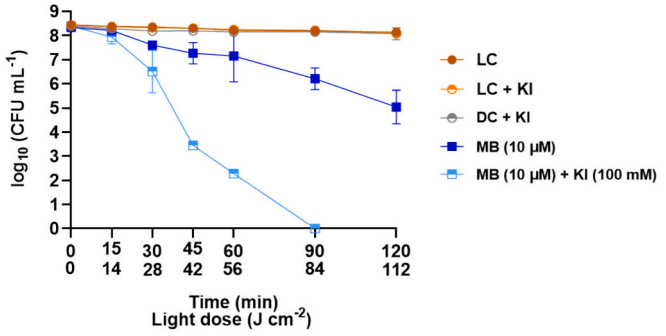

Fig. 4. Photodynamic inactivation of a consortium of the five selected bacterial strains in urine mediated with **MB** at 10 μM, in the presence and absence of KI at 100 mM, under white light irradiation at an effective light irradiance of 15.5 mW cm^{-2} for 120 min (total light dose of 112 J cm^{-2}). Values are presented as the means of three independent assays in duplicate; standard deviation is represented by error bars. LC: light control; DC: dark control.

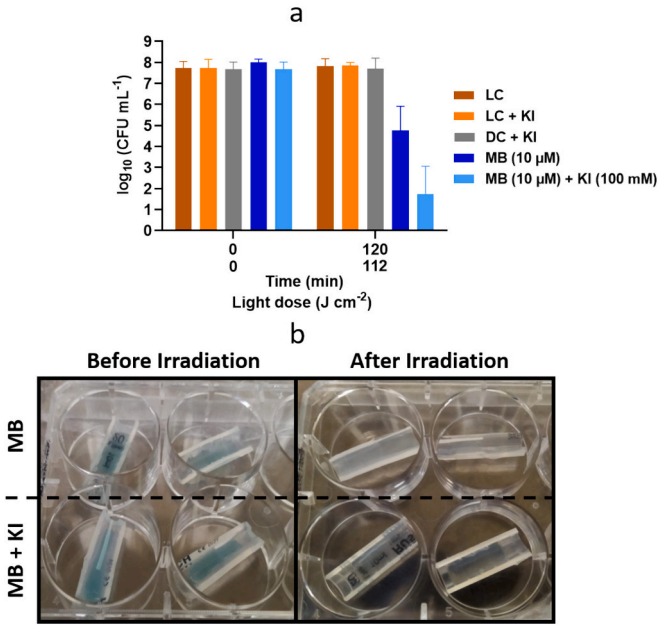

Fig. 5. a) Photodynamic inactivation of *E. coli* biofilms grown in TSB and treated with **MB** at 10 μM, in the presence and absence of KI at 100 mM, after 120 min of white light irradiation at an effective light irradiance of 15.5 mW cm^{-2} (total light dose of 112 J cm^{-2}). Values are presented as the means of three independent assays; standard deviation is represented by error bars. LC: light control; DC: dark control. b) Photographs of urinary catheters incubated with **MB** or **MB** + KI before and after 120 min of white-light exposure irradiation.

respectively (ANOVA, $p < 0.0001$). By comparison, a single **MB** + KI aPDT cycle yielded a reduction of 3.8 log_{10} CFU mL^{-1} (ANOVA, $p < 0.0001$), surpassing the cumulative effect of two **MB**-alone cycles. Two **MB**-aPDT + KI cycles resulted in a total *E. coli* reduction of 6 log_{10} CFU mL^{-1}.

4. Discussion

As mentioned above, aPDT emerges as a potential strategy to overcome microbial resistance associated with urinary infections [18]. Therefore, this study evaluated the potential of **MB**-mediated aPDT, alone and in combination with KI, to photoinactivate the five most prevalent UTI-causing bacteria in planktonic form. Additionally, the efficacy of the aPDT treatments was assessed in inhibiting *E. coli* biofilms

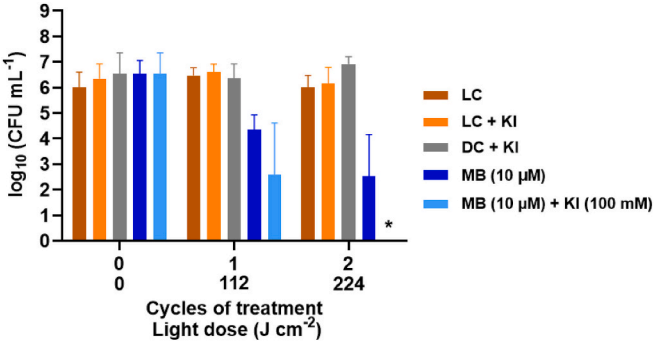

Fig. 6. Effect of two aPDT cycles (120 min each) on *E. coli* biofilms grown in urine. Treatments were performed with **MB** at 10 μM, in the presence and absence of KI at 100 mM, under white light irradiation at an effective irradiance of 15.5 mW cm^{-2} (total light dose: 112 J cm^{-2} for 1 cycle and 224 J cm^{-2} over 2 consecutive aPDT cycles). Values are presented as the means of three independent assays; standard deviation is represented by error bars. The asterisk (*) represents samples whose number of viable cells reached the method's detection limit. LC: light control; DC: dark control.

grown in urine and on catheter surfaces, which is particularly relevant since CAUTIs account for approximately 40% of all hospital-acquired infections [49].

MB was selected as the PS due to its extensive research history, proven efficacy, and clinical approval. KI was included in the aPDT assays due to its recognized enhancement of **MB** photodynamic activity, resulting in higher bacterial photoinactivation at shorter treatment times [27,28,47].

To establish conservative and reproducible experimental conditions, *P. aeruginosa,* widely regarded as one of the least susceptible bacterial species to aPDT, was used as the reference organism [47,48,50,54]. The preliminary *in vitro* assays conducted in PBS enabled the assessment of photodynamic performance in the absence of organic interference and defined standard conditions that were subsequently applied throughout the study, including *ex vivo* experiments. These preliminary aPDT experiments revealed that **MB** at 10 or 20 μM was an effective PS, capable of significantly reducing the concentration of *P. aeruginosa* viable cells by *ca.* 7 log_{10} CFU mL^{-1} after 120 min of white light exposure at an effective irradiance of 15.5 mW cm^{-2} (Fig. 2). These results align with previous studies showing that **MB** effectively photoinactivates Gram-negative bacteria due to its high ability to generate $^1O_2$ ($\varphi_\Delta = 0.52$) and strong affinity for bacterial cells [29,55]. The latter feature is attributed to the PS's cationic charge, which enables electrostatic binding to the negatively charged lipopolysaccharides (LPS) of the bacterial cell outer membrane [56]. This interaction displaces divalent cations in the LPS structure, creating gaps that facilitate close interaction of the PS with the bacterial cell wall [56]. Increasing the **MB** concentration from 10 to 20 μM did not yield statistically higher bacterial inactivation. This is likely attributable to concentration-dependent molecular aggregation *via* π-stacking of the phenothiazinium core, which can both reduce the ability of the **MB** to generate $^1O_2$ and limit effective light penetration through the solution owing to its high optical density [57]. Therefore, the minimum effective dose of 10 μM was selected to minimize potential systemic toxicity and formulation costs.

Combined **MB** + KI treatments were even more effective, achieving total bacterial inactivation (8.0 log_{10} CFU mL^{-1}) in a significantly shorter irradiation time of 15 min (Fig. 2) [25,27–29,32,33,43,58]. As mentioned above, this improved activity can be attributed to the action of reactive iodine species (RIS) generated in the presence of $^1O_2$ and KI, affording peroxyiodide ($HOOI_2^-$), which can undergo further decomposition *via* two different pathways: i) formation of free iodine/triiodide (I_2/I_3^-) and hydrogen peroxide (H_2O_2) and ii) formation of iodine radicals ($I_2^{\bullet-}$) *via* homolytic cleavage. Free iodine is a long-lived species and requires a sufficient threshold concentration to be bactericidal, while

iodine radicals act close to the target cells due to their short lifespan and limited diffusion. The shape of the microbial inactivation curves can provide insight into the dominant inactivation mechanism: a sharp decline is indicative of free iodine activity, whereas a more gradual decrease suggests the involvement of short-lived iodine radicals [26]. In our assays with KI (Fig. 2), the sharp photoinactivation profile observed suggests that free iodine (I_2/I_3^-) was the most relevant bactericidal species involved in *P. aeruginosa* photoinactivation, which is consistent with previous findings, also confirmed by UV/VIS spectrophotometry [27].

The aPDT assays performed in urine, a more physiologically relevant experimental medium for urinary tract infection-related studies than PBS, assessed the effectiveness of **MB**-mediated aPDT, alone or combined with KI, against each of the five most prevalent UTI-causing bacteria in the planktonic form, as well as against their combined five-strain mixture. **MB** was tested at a concentration of 10 μM, since higher concentrations showed no additional benefit in preliminary PBS assays. The findings indicated that **MB** alone was effective in aPDT treatments against most individual strains (> 3.0 $\log_{10}$ CFU mL^{-1} after 120 min of white light exposure), except *P. aeruginosa* and *K. pneumoniae* (Fig. 3). In contrast, the combined **MB** + KI aPDT treatment was effective against all five bacteria, significantly increasing the photoinactivation rate and decreasing the treatment time. When comparing bacterial susceptibility, *P. aeruginosa* was the most difficult bacterium to photoinactivate, followed by *K. pneumoniae*, *E. coli*, and *P. mirabilis*, while *E. faecalis,* the only Gram-positive bacterium*,* was the most sensitive. This difference can be attributed to structural and compositional differences between Gram-positive and Gram-negative organisms [59,60]. Gram-positive bacteria have a relatively porous cell wall, which leads to greater permeability and, therefore, easier penetration of PS into the cells. In contrast, Gram-negative bacteria have an additional outer membrane in their cellular structure, which contains LPS, phospholipids, lipoproteins, and proteins with porin function, forming a highly impermeable lipid structure [59,60]. Thus, the double-layer cell wall of Gram-negative bacteria acts as a barrier to PS, making them less susceptible to aPDT compared to Gram-positive bacteria [23,24].

The lowest susceptibility of *P. aeruginosa* among the Gram-negative bacteria to treatment can be associated with its outer membrane, which acts as a strong permeability barrier. According to literature, its permeability for antibiotics is only 8% of that of *E. coli*, largely due to the presence of porins that only allow the diffusion of small molecules with a molecular mass $\leq$ 200 Da [61]. The absence of larger general diffusion porins, such as OmpF and OmpC, present in *Enterobacteriaceae*, further contributes to the low permeability of *P. aeruginosa*'s outer membrane [61]. In *Pseudomonas*, the porin responsible for the formation of large channels is OprF; however, only a fraction of these pores remains open, limiting PS penetration through the cell wall and, consequently, bacterial inactivation [61].

Comparing the photoinactivation results of *P. aeruginosa* in PBS and urine (Figs. 2 and 3), it is evident that both aPDT treatments (**MB** and **MB** + KI) were less effective in the second matrix ($p < 0.05$, ANOVA). Urine is rich in organic matter [62], which can act as a scavenger of the ROS produced by **MB**, thereby limiting oxidative damage to the bacterial membrane [63]. Moreover, urine contains high concentrations of salts [62], which may influence aPDT treatment efficacy [29]. Previous studies have shown that salts such as NaBr, KCl, and NaCl can delay $^1O_2$ generation, thereby reducing the PS effectiveness [27].

In assays using the combined five-strain mixture, the aPDT treatment reduced the total bacteria concentration by more than 3.0 $\log_{10}$ CFU mL^1 after 120 min with **MB** alone and to the detection limit of the method with **MB** + KI, corresponding to 8.1 $\log_{10}$ CFU mL^{-1} reduction after 90 min of treatment (Fig. 4). These results indicate that aPDT is not only effective at inactivating individual bacteria but is also promising for controlling polymicrobial infections, which, although relatively rare, can occur under certain conditions such as long-term catheter use [64]. However, given that only planktonic cells of the five-strain mixture were tested in this study, evaluating the efficacy of this approach against polymicrobial biofilms represents an important direction for future research.

Urinary tract infections can be caused by planktonic microorganisms in urine, but significant proportions are linked with bacterial biofilms on urinary catheters [8]. Therefore, this study evaluated the potential of **MB**-mediated aPDT to destroy *E. coli* biofilms on catheters, as this bacterium is the main causative agent of such infections [5,6,9]. The aPDT treatments with **MB** and **MB** + KI effectively reduced the bacterial load within the biofilms (Fig. 5a). However, the combined treatment with KI was significantly more effective, achieving a 6.0 $\log_{10}$ CFU mL^{-1} reduction, twice the inactivation observed with **MB** alone (reduction of 3.0 $\log_{10}$ CFU mL^{-1}). Through these experiments, **MB** gradually photobleached (Fig. 5b), indicating degradation mediated by ROS [65,70]. Although this photobleaching reduces **MB** photodynamic efficacy, it could be advantageous in clinical settings by eliminating the need for **MB** removal post-treatment [58,65,70]. To counteract **MB** degradation, multiple treatment cycles could be applied, like conventional antimicrobial therapies that require multiple doses.

The efficacy of **MB** and **MB** + KI-mediated aPDT treatments against biofilms formed on catheters in urine was evaluated to simulate a more clinically relevant scenario. As observed for planktonic cells, bacterial photoinactivation in this medium after 120 min was reduced, reaching 2.1 and 3.8 $\log_{10}$ CFU mL^{-1} for **MB** and **MB** + KI, respectively. To enhance the aPDT efficiency under these conditions, the impact of a second aPDT cycle was assessed. The application of two consecutive aPDT cycles demonstrated a significant increase in biofilm photoinactivation, resulting in reductions of 3.4 and 6.0 $\log_{10}$ CFU mL^{-1} for **MB** and **MB** + KI, respectively (Fig. 6). These results demonstrate that repeated aPDT cycles can partially overcome the limitations imposed by complex matrices (urine) and support the potential of aPDT for biofilm control on urinary catheters.

When comparing the efficacy of two aPDT treatments (**MB** and **MB** + KI) against planktonic cells and biofilms formed in urine, a clear disparity in susceptibility is observed. Under identical aPDT treatment conditions (a single 120 min aPDT cycle), biofilms exhibited markedly lower reduction in bacterial concentration (2.1 and 3.8 $\log_{10}$ CFU mL^{-1}, for **MB** and **MB** + KI, respectively) than planktonic cells (3.2 and 8.0 $\log_{10}$ CFU mL^{-1}, respectively). Two aPDT cycles using either **MB** or **MB** + KI were required to achieve comparable reductions in bacterial load in biofilms and planktonic cells. These results indicate that bacteria in biofilms are inherently more difficult to photoinactivate than planktonic bacteria, in agreement with previous studies [40,66,67]. In fact, biofilms are complex 3D structures composed of bacterial cells embedded within an extracellular matrix rich in polysaccharides and proteins. This matrix acts as a physical and diffusional barrier, limiting the PS and light penetration and thereby reducing their access to cells located within the biofilm matrix [47,68]. Moreover, O_2 levels can be significantly lower within the biofilm than in the surrounding environment. A low-oxygen environment limits the formation of the highly reactive species $^1O_2$ produced during aPDT, which may contribute to the decreased effectiveness of aPDT in biofilms [34,69,70].

Previous studies have also demonstrated the effectiveness of other PSs in destroying bacterial biofilms on the surface of catheters. Recently, Misba and Khana demonstrated that impregnation of Toluidine Blue O (**TBO**) in urinary catheters was effective in eliminating *Staphylococcus aureus* biofilms (reduction of 6.0 $\log_{10}$ CFU mL^{-1}) [37]. This effect was observed after exposing silicone catheters to a **TBO** concentration of 700 μM, followed by irradiation with an LED lamp (light dose of 192.6 J cm^{-2}). Moreover, Santos and co-workers reported that a tetracationic porphyrin–cisplatin complex (**3-*cis*-PtTPyP**) at 10.72 μM reduced the concentration of *Proteus mirabilis* biofilms by 77% (0.64 $\log_{10}$ CFU mL^{-1}) on urinary catheters under white light irradiation (light dose of 360 J cm^{-2}) [36]. However, in the present study, **MB** + KI aPDT treatments were even more noteworthy, achieving a 6 $\log_{10}$ CFU mL^{-1} (99.9999%) reduction in biofilms grown in TSB after 120 min of white light exposure

(total light dose of 112 J cm^{-2}) and in urine after two aPDT cycles of 120 min (total light dose of 224 J cm^{-2}) using a lower **MB** concentration (10 μM). These results indicate comparable or superior antibiofilm efficacy while requiring reduced amounts of the PS, which is already commercially available and clinically approved. The use of lower **MB** concentration contributes to lower toxicity and lower aPDT treatment costs.

Taken together, these findings support **MB** + KI-mediated aPDT as a viable approach for reducing bacterial burden in complex matrices relevant to UTIs. Beyond its therapeutic application (involving **MB** + KI intravesical instillation, brief dark incubation and photoactivation), immobilization of **MB** on catheter surfaces combined with KI supplementation may provide a promising prophylactic strategy to prevent biofilm formation and catheter-associated UTIs. Catheter-associated infections are a particularly compelling target, since the window of opportunity for prophylactic intervention, before an established biofilm renders treatment substantially less effective, is predictable and, in principle, accessible [8,37,40]. Realizing this potential will, however, require further work on light delivery optimization within catheter geometries, formulation stability under storage conditions, and careful assessment of tolerance in urothelial tissue. None of these are trivial challenges, but the efficacy levels demonstrated here, particularly with repeated treatment cycles, justify pursuing them.

One limitation worth stating plainly is that biofilm photoinactivation was only evaluated for *E. coli*. While *E. coli* is the dominant uropathogen associated with CAUTIs [5,6,9], the susceptibility of biofilms formed by *K. pneumoniae*, *P. mirabilis*, *E. faecalis*, and *P. aeruginosa* individually and in combination remains to be determined. Extending the biofilm work to these species is a necessary step before broader claims about efficacy can be made, as well as polymicrobial biofilms, which remain an essential step for future investigations to confirm the broader generalizability of this treatment approach. Nevertheless, the overall findings of this study demonstrate that aPDT treatments mediated by **MB** and KI are effective in photoinactivating planktonic bacterial cells responsible for urinary infections and in significantly reducing bacterial cells within biofilms formed on urinary catheters, providing sufficient support for further preclinical evaluation of MB + KI-mediated aPDT as a strategy against CAUTIs.

5. Conclusion

In conclusion, the combination of **MB**-mediated aPDT with KI significantly enhances the antimicrobial efficacy of **MB**, enabling the reduction of less permeable bacteria such as *P. aeruginosa* and the effective control of mixed bacterial populations in urine. Moreover, under the experimental conditions evaluated, **MB** + KI-mediated aPDT effectively inactivated *E. coli* cells within biofilms on urinary catheter surfaces, suggesting its potential for the treatment of catheter-associated *E. coli* biofilms and for the decontamination of urinary catheter surfaces. Future studies should evaluate its efficacy against biofilms formed by other clinically relevant UTI pathogens, including *P. aeruginosa*, as well as polymicrobial biofilms associated with prolonged catheterization.

Animal and human rights statement

Not applicable (no living animals were used in this study).

CRediT authorship contribution statement

Daniela Silva: Writing – original draft, Visualization, Methodology, Investigation, Formal analysis, Data curation. **Inês Mendonça:** Writing – original draft, Visualization, Investigation, Formal analysis, Data curation. **Cátia Vieira:** Writing – original draft, Visualization, Validation, Investigation, Formal analysis, Data curation. **M. Graça P.M.S. Neves:** Writing – review & editing, Validation. **M. Amparo Faustino:** Writing – review & editing, Supervision, Resources, Project administration, Funding acquisition, Conceptualization. **Maria Bartolomeu:** Writing – review & editing, Validation, Supervision, Conceptualization. **Adelaide Almeida:** Writing – review & editing, Validation, Supervision, Resources, Project administration, Funding acquisition, Conceptualization.

Funding

This work received financial support from FCT/MECI (Fundação para a Ciência e a Tecnologia and Ministério da Educação, Ciência e Inovação) through the Centro de Estudos do Ambiente e do Mar (CESAM) (UID/50006 + LA/P/0094/2020, DOI: 10.54499/LA/P/0094/2020) and Laboratório Associado para a Química Verde Tecnologias e Processos Limpos (LAQV-REQUIMTE) (UID/50006/2025, DOI: 10.54499/UID/50006/2025).

Declaration of competing interest

The authors declare that they have no known competing financial interests or personal relationships that could have appeared to influence the work reported in this paper.

Acknowledgments

The authors thank the University of Aveiro and FCT/MECI (Fundação para a Ciência e a Tecnologia and Ministério da Educação, Ciência e Inovação) for the financial support for LAQV-REQUIMTE and CESAM. Cátia Vieira thanks FCT for her PhD grant (SFRH/BD/150358/2019).

Data availability

Data will be made available on request.

References

[1] N.S. Sheerin, Urinary tract infection, Medicine 39 (2011) 384–389, https://doi.org/10.1016/j.mpmed.2011.04.003.
[2] N. Sihra, S. Malde, T. Greenwell, M. Pakzad, M. Kujawa, A. Sinclair, Management of recurrent urinary tract infections in women, J Clin Urol 15 (2022) 152–164, https://doi.org/10.1177/2051415820939456.
[3] A. Silva, E. Costa, A. Freitas, A. Almeida, Revisiting the frequency and antimicrobial resistance patterns of bacteria implicated in community urinary tract infections, Antibiotics 11 (2022) 768, https://doi.org/10.3390/antibiotics11060768.
[4] T. Brooks, C.W. Keevil, A simple artificial urine for the growth of urinary pathogens, Lett. Appl. Microbiol. 24 (1997) 203–206, https://doi.org/10.1046/j.1472-765X.1997.00378.x.
[5] M.R. Asadi Karam, M. Habibi, S. Bouzari, Urinary tract infection: pathogenicity, antibiotic resistance and development of effective vaccines against Uropathogenic Escherichia coli, Mol. Immunol. 108 (2019) 56–67, https://doi.org/10.1016/j.molimm.2019.02.007.
[6] D.S. Lee, S.-J. Lee, H.-S. Choe, Community-acquired urinary tract infection by *Escherichia coli* in the era of antibiotic resistance, Biomed. Res. Int. 2018 (2018) 1–14, https://doi.org/10.1155/2018/7656752.
[7] A.L. Flores-Mireles, J.N. Walker, M. Caparon, S.J. Hultgren, Urinary tract infections: epidemiology, mechanisms of infection and treatment options, Nat. Rev. Microbiol. 13 (2015) 269–284, https://doi.org/10.1038/nrmicro3432.
[8] L.D. Dias, L.S. Duarte, P.L.F. Naves, H.B. Napolitano, V.S. Bagnato, Self-disinfecting urethral catheter to overcome urinary infections: from antimicrobial photodynamic action to antibacterial biochemical entities, Microorganisms 10 (2022) 2484, https://doi.org/10.3390/microorganisms10122484.
[9] M. Alshammari, A. Ahmad, M. AlKhulaifi, D. Al Farraj, S. Alsudir, M. Alarawi, et al., Reduction of biofilm formation of Escherichia coli by targeting quorum sensing and adhesion genes using the CRISPR/Cas9-HDR approach, and its clinical application on urinary catheter, J. Infect. Public Health 16 (2023) 1174–1183, https://doi.org/10.1016/j.jiph.2023.05.026.
[10] P. Tenke, T. Mezei, I. Bőde, B. Köves, Catheter-associated urinary tract infections, Eur. Urol. Suppl. 16 (2017) 138–143, https://doi.org/10.1016/j.eursup.2016.10.001.
[11] M. Lobanovska, G. Pilla, Penicillin's discovery and antibiotic resistance: lessons for the future? Yale J. Biol. Med. 90 (2017) 135–145.
[12] A.H. Holmes, L.S.P. Moore, A. Sundsfjord, M. Steinbakk, S. Regmi, A. Karkey, et al., Understanding the mechanisms and drivers of antimicrobial resistance, Lancet 387 (2016) 176–187, https://doi.org/10.1016/S0140-6736(15)00473-0.

[13] F. Al-Sarraj, The effect of antibiotics and photodynamic therapy on extended-spectrum beta-lactamase (ESBL) positive of Escherichia coli and Klebsiella pneumoniae in urothelial cells, Saudi J. Biol. Sci. 28 (2021) 5561–5567, https://doi.org/10.1016/j.sjbs.2021.05.074.
[14] A.S. Garcez, M. Kaplan, G.J. Jensen, F.R. Scheidt, E.M. Oliveira, S.S. Suzuki, Effects of antimicrobial photodynamic therapy on antibiotic-resistant Escherichia coli, Photodiagn. Photodyn. Ther. 32 (2020) 102029, https://doi.org/10.1016/j.pdpdt.2020.102029.
[15] E. Alves, M.A. Faustino, M.G. Neves, A. Cunha, J. Tome, A. Almeida, An insight on bacterial cellular targets of photodynamic inactivation, Future Med. Chem. 6 (2014) 141–164, https://doi.org/10.4155/fmc.13.211.
[16] A. Tavares, C.M.B. Carvalho, M.A. Faustino, M.G.P.M.S. Neves, J.P.C. Tomé, A. C. Tomé, et al., Antimicrobial photodynamic therapy: study of bacterial recovery viability and potential development of resistance after treatment, Mar. Drugs 8 (2010) 91–105, https://doi.org/10.3390/md8010091.
[17] S. Kwiatkowski, B. Knap, D. Przystupski, J. Saczko, E. Kędzierska, K. Knap-Czop, et al., Photodynamic therapy – mechanisms, photosensitizers and combinations, Biomed. Pharmacother. 106 (2018) 1098–1107, https://doi.org/10.1016/j.biopha.2018.07.049.
[18] G. Jori, M. Camerin, M. Soncin, L. Guidolin, O. Coppellotti, Chapter 1. Antimicrobial photodynamic therapy: basic principles, 2011, pp. 1–18, https://doi.org/10.1039/9781849733083-00001.
[19] F. Giuliani, M. Martinelli, A. Cocchi, D. Arbia, L. Fantetti, G. Roncucci, *In vitro* resistance selection studies of RLP068/Cl, a new Zn(II) phthalocyanine suitable for antimicrobial photodynamic therapy, Antimicrob. Agents Chemother. 54 (2010) 637–642, https://doi.org/10.1128/AAC.00603-09.
[20] I. Mendonça, D. Silva, T. Conde, T. Maurício, H. Cardoso, H. Pereira, et al., Insight into the efficiency of microalgae' lipidic extracts as photosensitizers for antimicrobial photodynamic therapy against Staphylococcus aureus, J. Photochem. Photobiol. B Biol. 259 (2024) 112997, https://doi.org/10.1016/j.jphotobiol.2024.112997.
[21] M.Q. Mesquita, J.C. Dias, M.G.P.M.S. Neves, A. Almeida, M.A.F. Faustino, Revisiting current photoactive materials for antimicrobial photodynamic therapy, Molecules 23 (2018), https://doi.org/10.3390/molecules23102424.
[22] A. Preuß, L. Zeugner, S. Hackbarth, M.A.F. Faustino, M.G.P.M.S. Neves, J.A. S. Cavaleiro, et al., Photoinactivation of *Escherichia coli* (SURE2) without intracellular uptake of the photosensitizer, J. Appl. Microbiol. 114 (2013) 36–43, https://doi.org/10.1111/jam.12018.
[23] W. Zhou, L. Chen, H. Li, M. Wu, M. Liang, Q. Liu, et al., Membrane disruption-enhanced photodynamic therapy against gram-negative Bacteria by a peptide-photosensitizer conjugate, ACS Nano (2024), https://doi.org/10.1021/acsnano.4c05443.
[24] F.F. Sperandio, Y.-Y. Huang, M.R. Hamblin, Antimicrobial photodynamic therapy to kill gram-negative bacteria, Recent Pat. Antiinfect. Drug Discov. 8 (2014) 108–120, https://doi.org/10.2174/1574891X113089990012.
[25] M.R. Hamblin, Potentiation of antimicrobial photodynamic inactivation by inorganic salts, Expert Rev. Anti-Infect. Ther. 15 (2017) 1059–1069, https://doi.org/10.1080/14787210.2017.1397512.
[26] N.S. Gsponer, M.L. Agazzi, M.B. Spesia, E.N. Durantini, Approaches to unravel pathways of reactive oxygen species in the photoinactivation of bacteria induced by a dicationic fulleropyrrolidinium derivative, Methods 109 (2016) 167–174, https://doi.org/10.1016/j.ymeth.2016.05.019.
[27] C. Vieira, A.T.P.C. Gomes, M.Q. Mesquita, N.M.M. Moura, M.G.P.M.S. Neves, M.A. F. Faustino, et al., An insight into the potentiation effect of potassium iodide on aPDT efficacy, Front. Microbiol. 9 (2018), https://doi.org/10.3389/fmicb.2018.02665.
[28] D. Vecchio, A. Gupta, L. Huang, G. Landi, P. Avci, A. Rodas, et al., Bacterial photodynamic inactivation mediated by methylene blue and red light is enhanced by synergistic effect of potassium iodide, Antimicrob. Agents Chemother. 59 (2015) 5203–5212, https://doi.org/10.1128/AAC.00019-15.
[29] C. Vieira, M. Bartolomeu, C.J.P. Monteiro, J.L. Romalde, P.P. Gallego, M.G.P.M. S. Neves, et al., Cationic photosensitizers and potassium iodide: an innovative approach for enhanced photodynamic inactivation of pathogenic bacteria in aquaculture, Aquaculture 596 (2025) 741882, https://doi.org/10.1016/j.aquaculture.2024.741882.
[30] L.D. Costa, C. Vieira, S. Hackbarth, M.G.P.M.S. Neves, A. Almeida, M.A.F. Faustino, et al., Photodynamic inactivation of *Escherichia coli* and *Staphylococcus aureus* by cationic diketopyrrolopyrroles, Dyes Pigments 244 (2026), https://doi.org/10.1016/j.dyepig.2025.113101.
[31] S.R.D. Gamelas, M. Bartolomeu, C. Vieira, M.A.F. Faustino, J.P.C. Tomé, A. C. Tomé, et al., Bacterial photodynamic inactivation: eradication of *Staphylococcus aureus* and *Escherichia coli* mediated by pyridinium-pyrazolyl zinc(II) phthalocyanines, ACS Appl. Bio Mater. 7 (2024) 7748–7757, https://doi.org/10.1021/acsabm.4c01368.
[32] Y.-Y. Huang, A. Wintner, P.C. Seed, T. Brauns, J.A. Gelfand, M.R. Hamblin, Antimicrobial photodynamic therapy mediated by methylene blue and potassium iodide to treat urinary tract infection in a female rat model, Sci. Rep. 8 (2018) 7257, https://doi.org/10.1038/s41598-018-25365-0.
[33] L. Huang, A. El-Hussein, W. Xuan, M.R. Hamblin, Potentiation by potassium iodide reveals that the anionic porphyrin TPPS4 is a surprisingly effective photosensitizer for antimicrobial photodynamic inactivation, J. Photochem. Photobiol. B 178 (2018) 277–286, https://doi.org/10.1016/j.jphotobiol.2017.10.036.
[34] C. Vieira, M. Bartolomeu, P.P. Gallego, M.G.P.M.S. Neves, J.L. Romalde, M.A. F. Faustino, et al., Photodynamic inactivation mediated by TMPyP and potassium iodide: a promising strategy for vibrio anguillarum control in aquaculture, Dyes Pigments 254 (2026) 113981, https://doi.org/10.1016/j.dyepig.2026.113981.
[35] S. Liu, S. Qiao, L. Li, G. Qi, Y. Lin, Z. Qiao, et al., Surface charge-conversion polymeric nanoparticles for photodynamic treatment of urinary tract bacterial infections, Nanotechnology 26 (2015) 495602, https://doi.org/10.1088/0957-4484/26/49/495602.
[36] D.J. Clerici, C. Hahn da Silveira, B.A. Iglesias, R. Christ Vianna Santos, The first evidence of antibiofilm action of *Proteus mirabilis* with tetra-cationic porphyrins containing cisplatin by antimicrobial photodynamic therapy, Microb. Pathog. 174 (2023) 105859, https://doi.org/10.1016/j.micpath.2022.105859.
[37] L. Misba, A.U. Khan, Domestic LED bulb induced photodynamic effect of toluidine blue O-embedded silicone catheters against urinary tract infection, Photodiagn. Photodyn. Ther. 42 (2023) 103590, https://doi.org/10.1016/j.pdpdt.2023.103590.
[38] M.J. Bovis, S. Noimark, J.H. Woodhams, C.W.M. Kay, J. Weiner, W.J. Peveler, et al., Photosensitisation studies of silicone polymer doped with methylene blue and nanogold for antimicrobial applications, RSC Adv. 5 (2015) 54830–54842, https://doi.org/10.1039/C5RA09045H.
[39] P.-H. Chen, G.-H. Chen, W.-B. Tsai, Innovative polymeric coatings with dual antifouling and light-activated bactericidal functions for urinary catheter applications, Polymers (Basel) 16 (2024) 2974, https://doi.org/10.3390/polym16212974.
[40] H. Vögeling, N. Plenagl, B.S. Seitz, L. Duse, S.R. Pinnapireddy, E. Dayyoub, et al., Synergistic effects of ultrasound and photodynamic therapy leading to biofilm eradication on polyurethane catheter surfaces modified with hypericin nanoformulations, Mater. Sci. Eng. C 103 (2019) 109749, https://doi.org/10.1016/j.msec.2019.109749.
[41] Y. Siegman-Igra, T. Kulka, D. Schwartz, N. Konforti, The significance of polymicrobial growth in urine: contamination or true infection, Scand. J. Infect. Dis. 25 (1993) 85–91, https://doi.org/10.1080/00365549309169675.
[42] Y. Siegman-Igra, The significance of urine culture with mixed flora, Curr. Opin. Nephrol. Hypertens. 3 (1994) 656–659, https://doi.org/10.1097/00041552-199411000-00017.
[43] X. Wen, X. Zhang, G. Szewczyk, A. El-Hussein, Y.-Y. Huang, T. Sarna, et al., Potassium iodide potentiates antimicrobial photodynamic inactivation mediated by Rose Bengal in *in vitro* and *in vivo* studies, Antimicrob. Agents Chemother. 61 (2017), https://doi.org/10.1128/AAC.00467-17.
[44] F.A. Schaberle, Assessment of the actual light dose in photodynamic therapy, Photodiagn. Photodyn. Ther. 23 (2018) 75–77, https://doi.org/10.1016/j.pdpdt.2018.06.009.
[45] I. Silva, M. Tacão, R.D.S. Tavares, R. Miranda, S. Araújo, C.M. Manaia, et al., Fate of cefotaxime-resistant Enterobacteriaceae and ESBL-producers over a full-scale wastewater treatment process with UV disinfection, Sci. Total Environ. 639 (2018) 1028–1037, https://doi.org/10.1016/j.scitotenv.2018.05.229.
[46] A. Vieira, Y.J. Silva, Â. Cunha, N.C.M. Gomes, H.-W. Ackermann, A. Almeida, Phage therapy to control multidrug-resistant Pseudomonas aeruginosa skin infections: in vitro and ex vivo experiments, Eur. J. Clin. Microbiol. Infect. Dis. 31 (2012) 3241–3249, https://doi.org/10.1007/s10096-012-1691-x.
[47] L. Huang, G. Szewczyk, T. Sarna, M.R. Hamblin, Potassium iodide potentiates broad-spectrum antimicrobial photodynamic inactivation using photofrin, ACS Infect Dis 3 (2017) 320–328, https://doi.org/10.1021/acsinfecdis.7b00004.
[48] N. Ignatova, T. Ivanova, A. Antonyan, I. Budruev, O. Streltsova, V. Elagin, et al., Efficacy of photodynamic inactivation against the major human antibiotic-resistant uropathogens, Photonics 8 (2021) 495, https://doi.org/10.3390/photonics8110495.
[49] T.L. Vollmerhausen, A. Conneely, C. Bennett, V.E. Wagner, J.C. Victor, C. P. O'Byrne, Visible and UVA light as a potential means of preventing Escherichia coli biofilm formation in urine and on materials used in urethral catheters, J. Photochem. Photobiol. B 170 (2017) 295–303, https://doi.org/10.1016/j.jphotobiol.2017.04.018.
[50] Y. Nitzan, M. Gutterman, Z. Malik, B. Ehrenberg, Inactivation of gram-negative bacteria by photosensitized porphyrins, Photochem. Photobiol. 55 (1992) 89–96, https://doi.org/10.1111/j.1751-1097.1992.tb04213.x.
[51] Y.-Y. Huang, H. Choi, Y. Kushida, B. Bhayana, Y. Wang, M.R. Hamblin, Broad-Spectrum antimicrobial effects of photocatalysis using titanium dioxide nanoparticles are strongly potentiated by addition of potassium iodide, Antimicrob. Agents Chemother. 60 (2016) 5445–5453, https://doi.org/10.1128/AAC.00980-16.
[52] Y.H. Cho, S.J. Lee, J.Y. Lee, S.W. Kim, I.C. Kwon, S.Y. Chung, et al., Prophylactic efficacy of a new gentamicin-releasing urethral catheter in short-term catheterized rabbits, BJU Int. 87 (2001) 104–109, https://doi.org/10.1046/J.1464-410X.2001.00978.X;WGROUP:STRING:PUBLICATION.
[53] A. Asséré, N. Oulahal, B. Carpentier, Comparative evaluation of methods for counting surviving biofilm cells adhering to a polyvinyl chloride surface exposed to chlorine or drying, J. Appl. Microbiol. 104 (2008) 1692–1702, https://doi.org/10.1111/J.1365-2672.2007.03711.X.
[54] M.N. Usacheva, M.C. Teichert, M.A. Biel, Comparison of the methylene blue and toluidine blue photobactericidal efficacy against gram-positive and gram-negative microorganisms, Lasers Surg. Med. 29 (2001) 165–173, https://doi.org/10.1002/lsm.1105.
[55] F. Wilkinson, W.P. Helman, A.B. Ross, Quantum yields for the photosensitized formation of the lowest electronically excited singlet state of molecular oxygen in solution, J. Phys. Chem. Ref. Data Monogr. 22 (1993) 113–262, https://doi.org/10.1063/1.555934.
[56] S. George, M.R. Hamblin, A. Kishen, Uptake pathways of anionic and cationic photosensitizers into bacteria, Photochem. Photobiol. Sci. 8 (2009) 788–795, https://doi.org/10.1039/b809624d.

[57] G. Szewczyk, K. Mokrzyński, Concentration-dependent photoproduction of singlet oxygen by common photosensitizers, Molecules 30 (2025), https://doi.org/10.3390/molecules30051130.
[58] Y. Zhang, T. Dai, M. Wang, D. Vecchio, L.Y. Chiang, M.R. Hamblin, Potentiation of antimicrobial photodynamic inactivation mediated by a cationic fullerene by added iodide: *in vitro* and *in vivo* studies, Nanomedicine 10 (2015) 603–614, https://doi.org/10.2217/nnm.14.131.
[59] A. Rapacka-Zdończyk, A. Woźniak, K. Michalska, M. Pierański, P. Ogonowska, M. Grinholc, et al., Factors determining the susceptibility of bacteria to antibacterial photodynamic inactivation, Front Med (Lausanne) 8 (2021), https://doi.org/10.3389/fmed.2021.642609.
[60] P. Niu, J. Dai, Z. Wang, Y. Wang, D. Feng, Y. Li, et al., Sensitization of antibiotic-resistant gram-negative bacteria to photodynamic therapy via perfluorocarbon nanoemulsion, Pharmaceuticals 15 (2022) 156, https://doi.org/10.3390/ph15020156.
[61] S. Chevalier, E. Bouffartigues, J. Bodilis, O. Maillot, O. Lesouhaitier, M.G. J. Feuilloley, et al., Structure, function and regulation of Pseudomonas aeruginosa porins, FEMS Microbiol. Rev. 41 (2017) 698–722, https://doi.org/10.1093/femsre/fux020.
[62] T.A. Larsen, M.E. Riechmann, K.M. Udert, State of the art of urine treatment technologies: a critical review, Water Res. X 13 (2021) 100114, https://doi.org/10.1016/j.wroa.2021.100114.
[63] V.T. Orlandi, E. Caruso, S. Banfi, P. Barbieri, Effect of organic matter on the *in vitro* Photoeradication of *Pseudomonas aeruginosa* by means of a cationic tetraaryl-porphyrin †, Photochem. Photobiol. 88 (2012) 557–564, https://doi.org/10.1111/j.1751-1097.2012.01122.x.
[64] B. Köves, A. Magyar, P. Tenke, Spectrum and antibiotic resistance of catheter-associated urinary tract infections, GMS Infect. Dis. 5 (2017) Doc06, https://doi.org/10.3205/id000032.
[65] I. Khan, K. Saeed, I. Zekker, B. Zhang, A.H. Hendi, A. Ahmad, et al., Review on methylene blue: its properties, uses, toxicity and photodegradation, Water 14 (2022) 242, https://doi.org/10.3390/w14020242.
[66] S. Beirão, S. Fernandes, J. Coelho, M.A.F. Faustino, J.P.C. Tomé, M.G.P.M.S. Neves, et al., Photodynamic inactivation of bacterial and yeast biofilms with a cationic porphyrin, Photochem. Photobiol. 90 (2014) 1387–1396, https://doi.org/10.1111/php.12331.
[67] L.M.O. Lourenço, D.M.G.C. Rocha, C.I.V. Ramos, M.C. Gomes, A. Almeida, M.A. F. Faustino, et al., Photoinactivation of planktonic and biofilm forms of *Escherichia coli* through the action of cationic zinc(II) phthalocyanines, ChemPhotoChem 3 (2019) 251–260, https://doi.org/10.1002/cptc.201900020.
[68] S. Pandit, M. Fazilati, K. Gaska, A. Derouiche, T. Nypelö, I. Mijakovic, et al., The Exo-polysaccharide component of extracellular matrix is essential for the viscoelastic properties of *Bacillus subtilis* biofilms, Int. J. Mol. Sci. 21 (2020) 6755, https://doi.org/10.3390/ijms21186755.
[69] M. Nie, J. Yang, A. Rastelli, Y. Shen, D. Deng, Oxygen availability on the application of antimicrobial photodynamic therapy against multi-species biofilms, Pathogens 12 (2023) 904, https://doi.org/10.3390/pathogens12070904.
[70] C. Vieira, M. Trigo, C.J. Dias, B. Bartolomeu, P.P. Gallego, M.G.P.M.S. Neves, et al., Photodynamic inactivation as a novel approach for seabass decontamination: effectiveness of TMPyP and methylene blue treatments, Food Bioprocess Technol. 18 (2025) 7112–7130, https://doi.org/10.1007/s11947-025-03869-8.